Supporting Information

Facile Engineering of Resveratrol Nanoparticles Loaded with 20(S)- Protopanaxadiol for the Treatment of Periodontitis by Regulating the Macrophage Phenotype

Huimin Huangfu [a, b], Shulin Du [c], Hao Zhang [a, b], Hanchi Wang [a, b], Yi Zhang [a, b], Zhen Yang [a, b], Xinwei Zhang [a, b], Sicong Ren [a, b], Siyu Chen [a, b], Cuizhu Wang [d *], Yidi Zhang [a, c *], Yanmin Zhou [a, b *]

[a] Department of Oral Implantology, Hospital of Stomatology, Jilin University, Changchun,130021, China

[b] Jilin Provincial Key Laboratory of Tooth Development and Bone Remodeling, Hospital of Stomatology, Jilin University, Changchun, 130021, China

[c] State Key of Supramolecular Structure and Materials, College of Chemistry, Jilin University Laboratory, Changchun 130012, China

[d] School of Pharmaceutical Sciences Jilin University, Changchun, 130021, China

Corresponding author:

Email: zhouym@jlu.edu.cn (Prof. Y. Zhou), zhangyidi@jlu.edu.cn (Dr. Y. Zhang), wangcuizhu@jlu.edu.cn (Dr. C. Wang).

Contents of the Supplementary Information

- Additional Experimental Methods
- Additional Table S1
- Additional Figures S1-S13 and notes

Table S1. Primer sequences were used in this study.

Figure S1. SEM images of RES NPs and RES@PPD NPs

Figure S2. The ^{1}H-NMR spectra of A) RES and B) RES NPs.

Figure S3. A) Image of Resveratrol and 20(S)- protopanaxadiol DMSO solution. The Resveratrol DMSO solution is on the left and the 20(S)- protopanaxadiol DMSO solution is on the right. B) Images of the synthesis process of RES NPs and RES@PPD NPs. RES NPs are on the left and RES@PPD NPs are on the right. C) Image of RES NPs and RES@PPD NPs end product. RES NPs

are on the left and RES@ PPD NPs are on the right.

Figure S4. XRD measurement of RES NPs and RES@PPD NPs

Figure S5. Photograph A) and particle sizes B) of RES@PPD NPs in deionized water, normal saline, PBS, and cell culture medium. Photograph C) and particle sizes D) of RES@PPD NPs in deionized water, normal saline, PBS, and cell culture medium after incubation for 7 days and gently shaking.

Figure S6. Thermogravimetric analysis (TGA) curves for PPD, RES, RES@PPD NPs.

Figure S7. Drug release of RES and PPD.

Figure S8. The intracellular ROS were analyzed by fluorescence intensity of DCF.

Figure S9. Uptake of FITC-labeled RES@PPD NPs was observed in two different cells by confocal microscopy and Flow cytometry studies.

Figure S10. TEM images of RAW 264.7 and L929 cells were processed by RES@PPD NPs.

Figure S11. The relative hemolysis rates of RES@PPD NPs (0,25,50,75,100 μg mL^{-1}) with different concentrations.

Figure S12. HGFs images were incubated with RES@PPD NPs at serial concentrations (0,25,50,75,100 μg mL^{-1}). HGFs without any treatment were used as the blank group.

Figure S13. The main organ sections of SD rats treated by subgingival injection of RES@PPD NPs were stained with H&E. Rats treated with PBS were used as a control group. After the local injection of RES@PPD NPs, the main organs were harvested 30 days later. The morphological changes of nanoparticles treated group are not obvious, which indicates that RES@PPD NPs had excellent biological safety *in vivo*.

1. *Additional Experimental Methods*

1.1. Entrapment Efficiency (EE) and Drug Loading (DL)

The drug content in the nanoparticles was assayed by HPLC (Agilent LC 1100, Santa Clara, CA, USA). A Venusil XBP C18 column（5μm,100Å,4.6×250 mm）was used. Accurately weigh RES@PPD NPs after vacuum drying for 24 hours to ensure that each sample contains the same quality of PPD. In order to simulate the physiological environment *in vivo*, RES@PPD NPs were immersed in PBS (PH=7.4, 0.5% Tween 80) and vibrated in a constant temperature water bath at 37 ℃, and the rotation speed was set at 100 rpm. At a specific time interval, take out 1 mL of the

release solution and replenish the same amount of fresh PBS solution. The released liquid was filtered by a filter membrane three times and then put into a liquid sample bottle. The flow rate of the mobile phase was 1 mL min^{-1}. The column effluent was detected at 295 nm with an ultraviolet/visible detector. Each group of samples was measured 3 times and averaged. The EE and DL were calculated with equations (1) and (2).

$$EE(\%) = \frac{W_{\text{Total}} - W_{\text{Free}}}{W_{\text{Total}}} \times 100\% \quad \text{.....(1)}$$

$$\text{DL}\ (\%) = \frac{W_{\text{Total}} - W_{\text{Free}}}{W_{\text{Drug}}} \times 100\% \quad \text{.....(2)}$$

1.2. *In Vitro* Drug Release

Briefly, 15 mg nanoparticles were dispersed in 5 mL of release medium phosphate buffer solution (PBS) or saline with 0.1% w/v tween 80 to form a suspension. Tween 80 was used to increase the solubility of RES and PPD in buffer solution and to avoid the combination of RES and PPD with the pipe wall. The suspension was put into a standard-grade regenerated cellulose dialysis membrane (Spectra/Por 6, MWCO = 1,000, Spectrum, Houston, TX, USA). Then, the closed bag was placed in a centrifuge tube and immersed in 15 mL of release medium. The test tube was placed in an orbital water bath and shaken at 37 ℃ at 120 rpm. At a given time interval, 10 mL samples were aspirated for analysis and replaced with fresh medium. In this study, *in vitro* release experiment, the sinking condition was maintained by adding Tween 80 and changing fresh buffer frequently. The analysis procedure was similar to the measurement of EE.

2. ***Additional Table S1***

Table S1. Primer sequences were used in this study.

Gene	Forward Sequence (5'to3')	Reverse Sequence (5'to3')
TNF-α	ACTCCAGGCGGTGCCTATGT	GTGAGGGTCTGGGCCATAGAA
IL-6	CCACTTCACAAGTCGGAGGCTTA	CCAGTTTGGTAGCATCCATCATTTC
IL-1β	TCCAGGATGAGGACATGAGCAC	GAACGTCACACACCAGCAGGTTA
IL-10	ATGCTGCCTGCTCTTACTGACTG	CCCAAGTAACCCTTA AAGTCCTGC
TGF-β	CTTCAGCCTCCACAGAGAAGAACT	TGTGTCCAGGCTCCAAATATAG
Arg-1	TGTGTCCAGGCTCCAAATATAG	AGCAGGTAGCTGAAGGTCTC

β-actin	CATCCGTAAAGACCTCTAGCCAAC	ATGGAGCCACCGATCCACA

3. ***Additional Figure S1-S13 and notes***

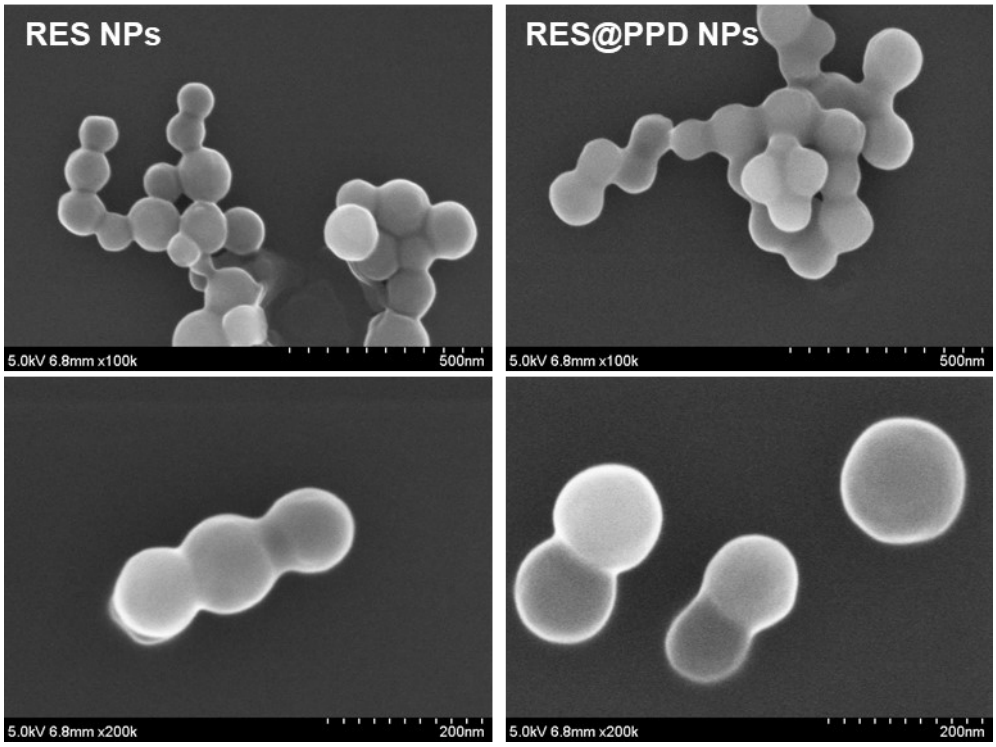

Figure S1. SEM images of RES NPs and RES@PPD NPs

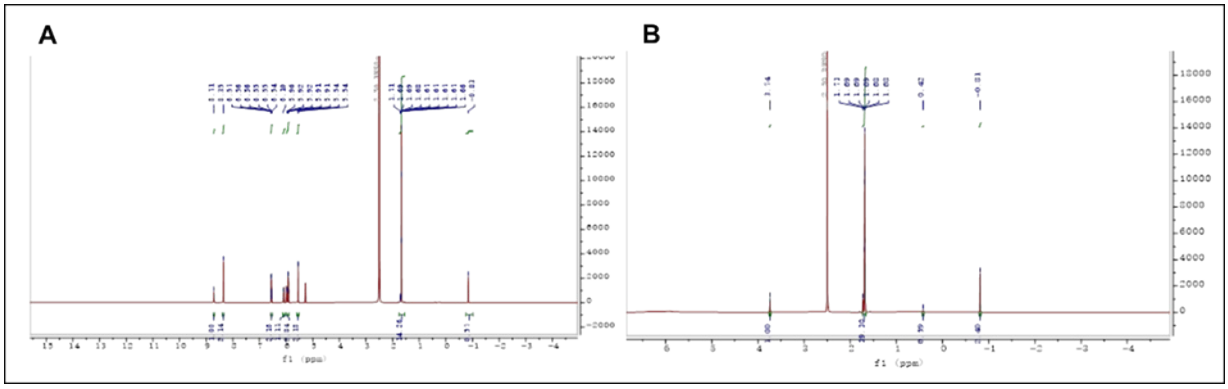

Figure S2. The ^{1}H-NMR spectra of A) RES and B) RES NPs.

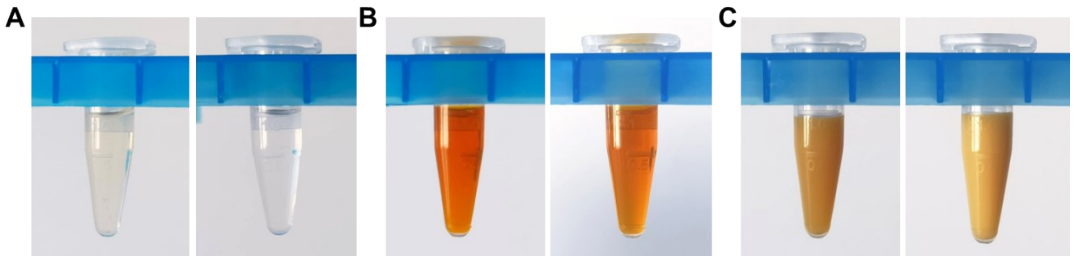

Figure S3. A) Image of Resveratrol and 20(S)- protopanaxadiol DMSO solution. The Resveratrol DMSO solution is on the left and the 20(S)- protopanaxadiol DMSO solution is on the right. B)

Images of the synthesis process of RES NPs and RES@PPD NPs. RES NPs are on the left and RES@PPD NPs are on the right. C) Image of RES NPs and RES@PPD NPs end product. RES NPs are on the left and RES@ PPD NPs are on the right.

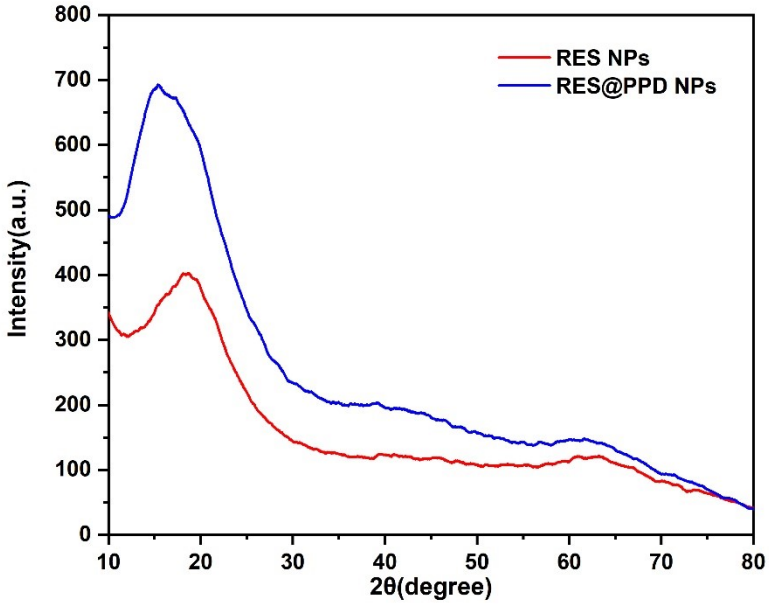

Figure S4. XRD measurement of RES NPs and RES@PPD NPs.

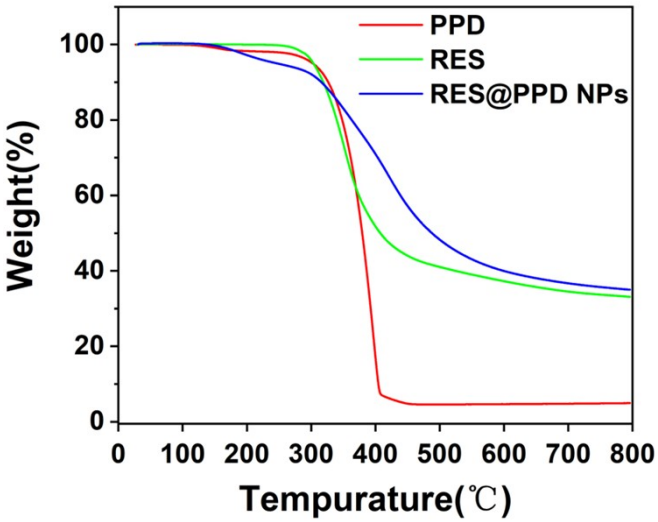

Figure S5. Thermogravimetric analysis (TGA) curves for PPD, RES, RES@PPD NPs.

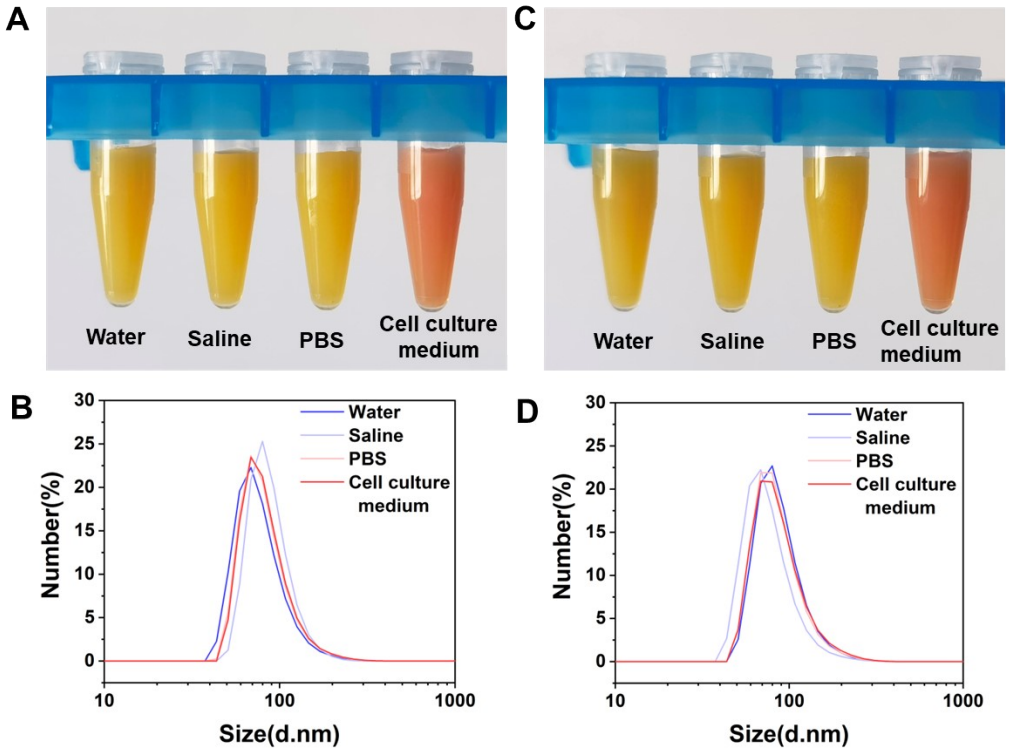

Figure S6. Photograph A) and particle sizes B) of RES@PPD NPs in deionized water, normal saline, PBS, and cell culture medium. Photograph C) and particle sizes D) of RES@PPD NPs in deionized water, normal saline, PBS, and cell culture medium after incubation for 7 days and gently shaking.

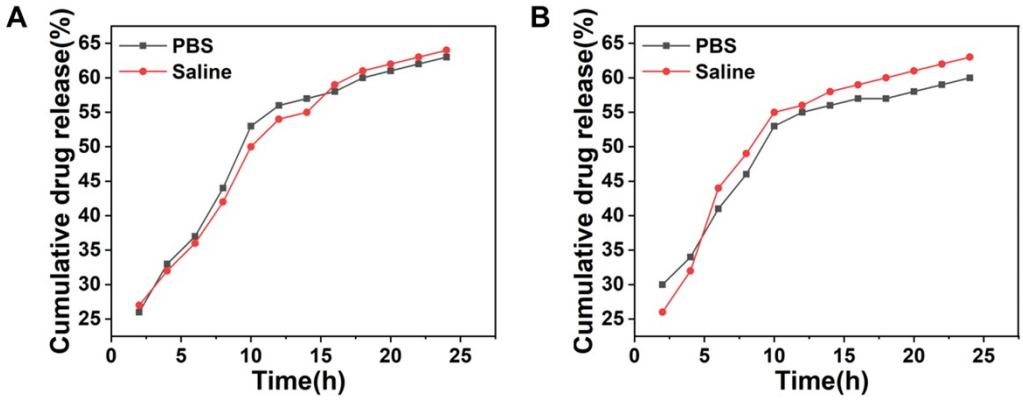

Figure S7. Drug release of RES and PPD**.**

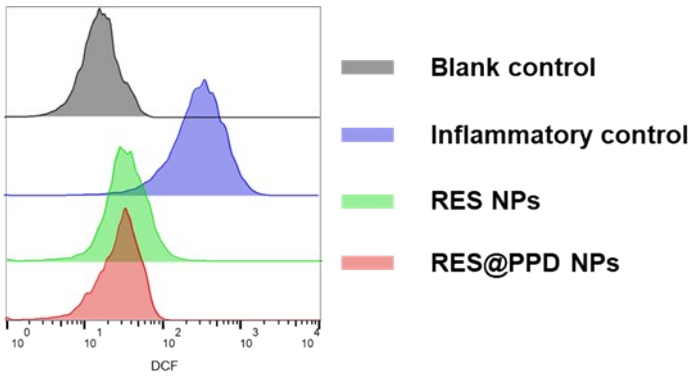

Figure S8. The intracellular ROS were analyzed by fluorescence intensity of DCF.

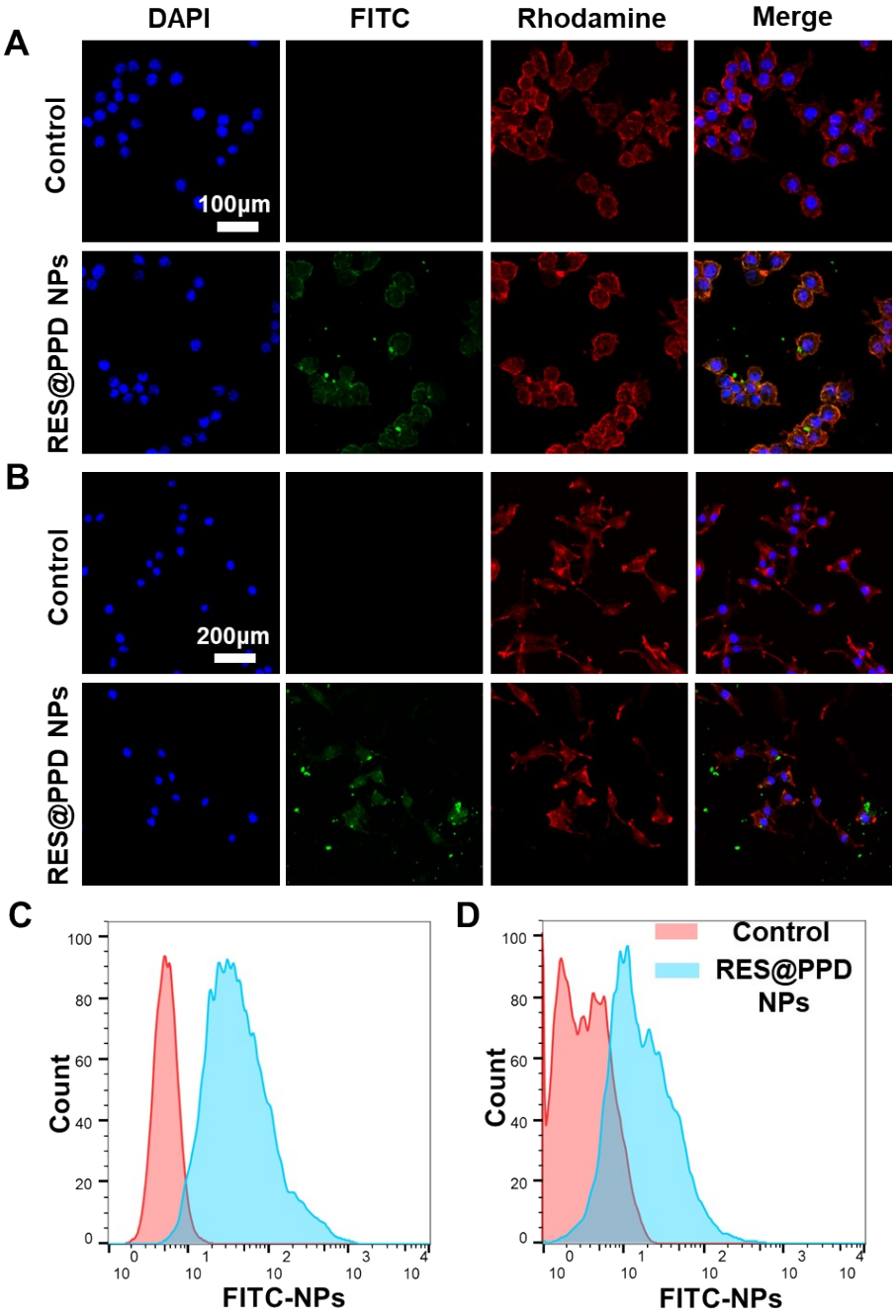

Figure S9. The uptake of FITC-labeled RES@PPD NPs was observed in two different cells by confocal microscopy and flow cytometry studies. Confocal microscopy images of A) RAW 264.7 and B) L929. The flow cytometry results of C) RAW 264.7 and D) L929. RAW 264.7 and L929 cells were incubated with a blank medium (control) and RES@PPD NPs for 4 hours, respectively. Cell nuclei were stained blue with DAPI, filamentous actin cytoskeletons were stained red with rhodamine-phalloidin, and FITC was green fluorescence.

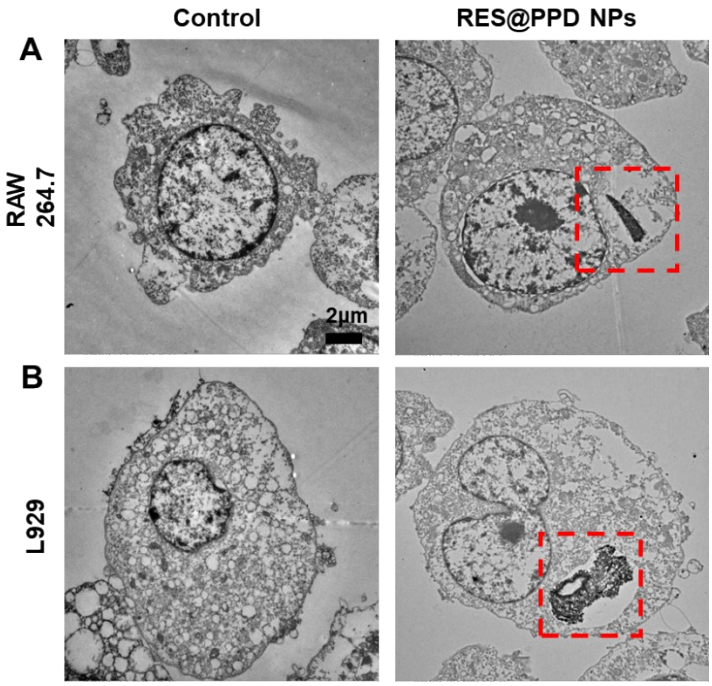

Figure S10. TEM images of RAW 264.7 and L929 cells were processed by RES@PPD NPs.

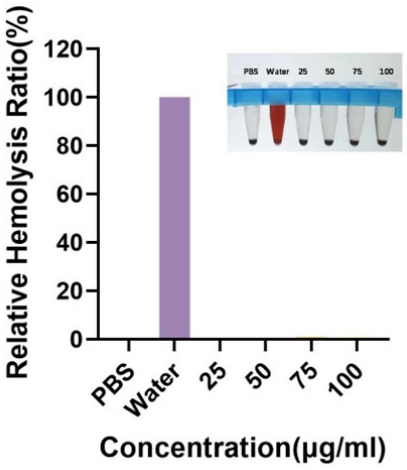

Figure S11. The relative hemolysis rates of RES@PPD NPs (0,25,50,75,100 μg mL^{-1}) with different concentrations.

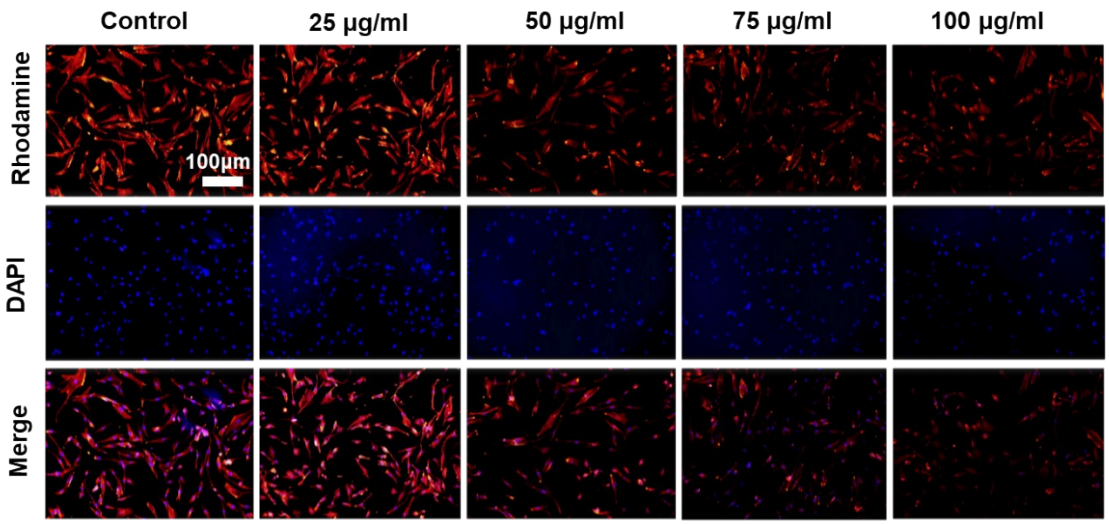

Figure S12. HGFs images were incubated with RES@PPD NPs at serial concentrations (0,25,50,75,100 μg mL^{-1}). HGFs without any treatment were used as the blank group.

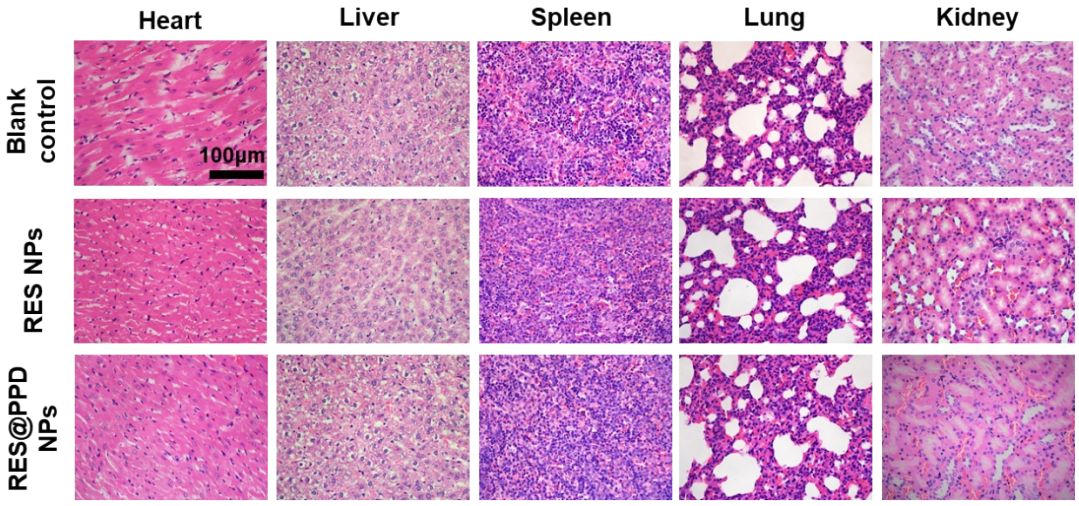

Figure S13. The main organ sections of SD rats treated by subgingival injection of RES@PPD NPs were stained with H&E. Rats treated with PBS were used as a control group. After the local injection of RES@PPD NPs, the main organs were harvested 30 days later. The morphological changes of nanoparticles treated group are not obvious, which indicates that RES@PPD NPs had great biological safety *in vivo*.